International Journal of Applied Pharmaceutics

ISSN- 0975-7058 Vol 18, Issue 2, 2026

Original Article

DOE-BASED FORMULATION AND CHARACTERIZATION OF NIFEDIPINE-LOADED SMEDDS EMBEDDED IN FAST DISSOLVING FILMS FOR IMPROVED ORAL BIOAVAILABILITY

DHANUSH R.[1], SUJATHA K.[2], PREETHIKA S.[3], SOWMYA C.[4*]

[1,3,4]Department of Pharmaceutics, Sri Ramachandra Faculty of Pharmacy, Sri Ramachandra Institute of Higher Education and Research (DU), Porur-600116, Chennai, Tamil Nadu, India. [2]Department of Pharmaceutical Chemistry, Sri Ramachandra Faculty of Pharmacy, Sri Ramachandra Institute of Higher Education and Research (DU), Porur-600116, Chennai, Tamil Nadu, India
*Corresponding author: Sowmya C.; *Email: drcsowmya@sriramachandra.edu.in

Received: 22 Oct 2025, Revised and Accepted: 12 Jan 2026

ABSTRACT

Objective: Nifedipine (NIFD), a calcium channel blocker with poor aqueous solubility and low oral bioavailability, requires formulation enhancement for effective delivery. This study aimed to develop and optimise a self-microemulsifying drug delivery system (SMEDDS) of NIFD and incorporate it into mouth-dissolving films (MDFs) to improve solubility, dissolution, and patient compliance.

Methods: Box-Behnken Design (BBD) was employed to optimise SMEDDS formulations using castor oil (A), Tween 80 (B), and Span 80 (C) as factors, with droplet size (Y1) and transmittance (%) as responses. The optimised SMEDDS batches (FS14-FS16) were characterised for droplet size, PDI, zeta potential, and transmittance and subsequently incorporated into MDFs (F1-F3) by solvent casting.

Results: The optimised SMEDDS exhibited droplet sizes between 196-201 nm, PDI values of 0.534-0.608, and zeta potentials from-15.66 to-21.07 mV, indicating nanoscale dispersion and moderate stability. The resulting SMEDDS-loaded films (F1-F3) showed uniform thickness (0.11-0.15 mm), rapid disintegration (48-60 s), and high drug content (87.04-95.08%). The diffusion of NIFD increased by a factor 3 after incorporating it into SMEDDS.

Conclusion: The optimised nifedipine-loaded SMEDDS (FS14-FS16) successfully incorporated into mouth-dissolving films (F1-F3), significantly enhanced solubility and dissolution. Among the MDFs, F1 emerged as the best, demonstrating superior *in vitro* drug release compared to the pure NIFD film, offering a promising oral delivery system for enhancing the bioavailability of poorly soluble drugs.

Keywords: SMEDDS, Bioavailability, Nifedipine, Mouth dissolving films, Wellbeing, Box-behnken design, Microemulsion

DOI: https://dx.doi.org/10.22159/ijap.2026v18i2.57227 Journal homepage: https://innovareacademics.in/journals/index.php/ijap

INTRODUCTION

Oral drug delivery systems are extensively recognised and are the most favoured route of pharmaceutical administration due to their convenience, ease of use, cost-effectiveness, and superior patient compliance [1, 2]. This mode of drug delivery encompasses a range of pharmaceutical formulations, including tablets, capsules, liquids, and more advanced systems such as MDFs [3, 4]. NIFD, a member of the dihydropyridine class of calcium channel blockers, has been predominantly recommended for the management of angina pectoris characterized by chest pain resulting from reduced myocardial blood flow and hypertension [5]. NIFD is classified as a Biopharmaceutical Classification System (BCS) Class II drug due to its limited aqueous solubility [6]. This solubility limitation poses a challenge to its dissolution in gastrointestinal fluids, thereby potentially reducing its bioavailability [7]. Various formulation strategies, including extended and immediate release systems, were designed to improve absorption and therapeutic efficacy of NIFD. In the present research, NIFD was converted to SMEDDS to improve its drug solubility and dissolution rate, thereby enhancing absorption and efficacy [8, 9].

The integration of SMEDDS with MDF presents an innovative approach to drug delivery by harnessing the advantages of both systems [10–12]. While MDF provides rapid drug release, ease of administration, and faster action [13]. This synergistic formulation holds the potential to conquer all limitations related to the conventional oral types of dosing, thereby improving therapeutic outcomes [14–16]. The objective of this work was to develop, optimise, and characterise an NIFD-SMEDDS and incorporate it into a mouth-dissolving film (MDF) to enhance solubility, dissolution rate, and patient acceptability. The study is novel in that it integrates a Box–Behnken optimised Nifedipine-loaded SMEDDS into a mouth-dissolving film, combining solubility enhancement with rapid drug release. This dual approach offers a patient-friendly system that improves oral bioavailability and therapeutic efficiency.

MATERIALS AND METHODS

Materials

Nifedipine (NIFD) was kindly provided by Ipca Laboratories Ltd., Maharashtra, India, as a gift sample. Polyvinylpyrrolidone (PVP K-30, analytical grade), Tween 80 (polyoxyethylene sorbitan monooleate, analytical grade), and Span 80 (sorbitan monooleate, analytical grade), all procured from Sisco Research Laboratories Pvt. Ltd., Chennai, India. Hydroxypropyl methylcellulose (HPMC E5, pharmaceutical grade) and Polyethylene glycol 400 (PEG 400, analytical grade) were obtained from Sigma-Aldrich Pvt. Ltd., Bangalore, India. Pharmaceutical-grade castor oil was sourced from Veda Oil Pvt. Ltd., Haryana, India. Additionally, sucrose (analytical grade) from HiMedia Laboratories Pvt. Ltd., Maharashtra, and citric acid (analytical grade) from Thermo Fisher Scientific India Pvt. Ltd., Maharashtra, were used in the formulations. Distilled water prepared in the laboratory served as the aqueous phase throughout the study.

Construction of pseudo-ternary phase diagram

The self-emulsifying area was determined by the construction of a pseudo-ternary phase diagram for a surfactant and co-surfactant mixture combination was constructed at 1:1 and 1:2 ratios [17, 18]. (Smix) (b), oil (a), and water (c) using Smix ratios from 9:1 to 1:9 using Chemix School software. The microemulsion zone was identified for each ratio from the pseudo-ternary phase diagram [19, 20].

Preparation and optimisation of NIFD SMEDDS using BBD

Optimisation of the SMEDDS was performed by employing a BBD with 13 experimental runs, FS1 to FS13, to assess the effect of formulation ingredients on key quality attributes [21]. Independent variables chosen were castor oil (A), Tween 80 (B), and Span 80 (C), each of which was investigated at three levels of concentration [22]. Castor oil was selected as the lipid phase owing to its superior nifedipine solubility, chemical stability, and regulatory acceptance

compared to medium-chain triglycerides (MCT), making it ideal for oral formulations. Tween 80 and Span 80 were employed as a surfactant–co-surfactant pair to achieve an optimal HLB (10–12), which promotes the formation of stable o/w microemulsions with long-chain triglycerides like castor oil. This combination has been previously reported to produce stable SMEDDS with nanosized droplets and improved solubility and bioavailability for poorly soluble drugs in oral delivery systems [23]. The key responses that were assessed were Droplet size (nm) (Y1) to determine the emulsification efficiency, and transmittance (%) (Y2), to find the stability and transparency of the SMEDDS. The impact of variables and how they interact with output variables has been analyzed using analysis of variance (ANOVA), and their relationship was studied using polynomial equations and represented as contour and response surface plots [24]. Finally, using the desirability function, optimized variables (FS14, FS15, and FS16) were determined to produce the SMEDDS with minimum droplet size and maximum transmittance. The SMEDDS formulation was developed by mixing (A), (B), and (C) to form a stable emulsion, followed by adding NIFD, sucrose, and citric acid [25–27]. Because NIFD is highly sensitive to light, all experiments were carried out in a darkened room [28, 29].

Integration optimized SMEDDS into MDFs

PVP and HPMC were dissolved in distilled water while being constantly stirred to create a polymer solution with PEG-400. The prepared SMEDDS was then gradually added to the polymer solution with continuous stirring to achieve a homogenous mixture [30, 31]. After being transferred to a Petri dish, this mixture was dried in a tray dryer. After drying, the film was carefully removed and cut into 2 × 2 cm^2 size and stored for further evaluation. Optimized three formulations (FS14-FS16) were integrated with MDFs (F1-F3), and one pure NIFD MDF (F4) was prepared and evaluated [32, 33]. The process of preparation of SMEDDS integrated MDF is shown in fig. 1.

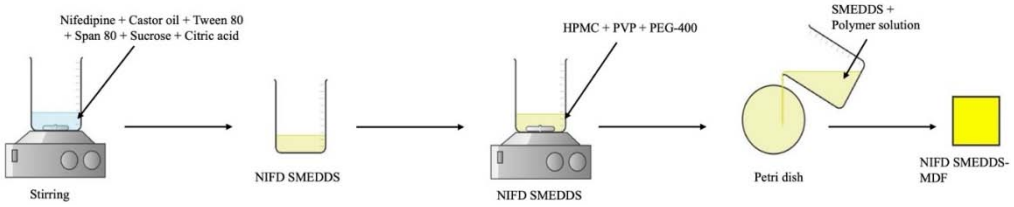

Fig. 1: Schematic illustration of the preparation of NIFD-loaded SMEDDS and their integration into MDFs

Evaluation of SMEDDS

Solubility

The solubility of pure NIFD and NIFD-loaded SMEDDS (FS14, FS15, and FS16) was determined in water using the shake flask method [34–36].

Droplet size, PDI, and Zeta potential

The droplet size, PDI, and Zeta potential of formulated SMEDDS, FS1-FS16, were measured using a Malvern Zetasizer [37–40]

Transmittance

The clarity of the SMEDDS formulation FS1-FS16 was assessed by measuring % transmittance using a UV-visible spectrophotometer at 650 nm [41–43].

Cloud point

Cloud point of SMEDDS Optimized formulation (FS14, FS15, and FS16) was measured to assess its thermal stability and phase behaviour after dilution. The formulation was diluted in distilled water (1:100) and was kept in a sealed glass vial. The sample was heated slowly in a temperature-controlled water bath under constant stirring. The temperature at which the clear solution became turbid (cloudy) was noted visually as the cloud point temperature [44, 45].

Dispersibility

Dispersibility of SMEDDS Optimized formulation (FS14, FS15, and FS16) was assessed by pouring 1 ml of the formulation into 500 ml of phosphate buffer pH 6.8 at 37±0.5 °C under gentle agitation at 50 rpm in a USP dissolution apparatus II. Emulsification time and type of emulsion produced were visually monitored and graded [46, 47]. The grade and observation are given in table 1.

Surface morphology studies of SMEDDS using SEM

Scanning Electron Microscopy (SEM) is employed to analyze the surface morphology of the F1 and F4 at specified magnifications [48, 49].

Table 1: Qualitative grading system for evaluating dispersibility and emulsification behaviour of optimised SMEDDS formulations

S. No.	Grade	Observation	Time
1.	A	Transparent or bluish appearance	Rapid formation (Less than 1 min)
2.	B	Less transparent, bluish-white appearance	Rapidly forming (Less than 1 min)
3.	C	Fine white milkish avant-garde Emulsion	Within 2 min
4.	D	Greyish white Emulsion	Slow emulsification process
5.	E	Large globules of oil are visible on the surface.	Slow emulsification process

FT-IR spectral analysis of SMEDDS

The SMEDDS-MDF induced due to polymer interactions was captured using the Bruker Alpha II FTIR spectrophotometer. Samples were scanned at 500–4000 cm-1 [50–52].

Evaluation of SMEDDS integrated MDFs (F1-F3) and plain NIFD film (F4)

pH

The pH of the surface MDF formulation F1-F4 was measured with a calibrated digital pH meter [53, 54].

Weight variation

Four films F1-F4 of the same size (usually 2×2 cm^2) were cut from different areas of the casted film. Each film was measured separately with an analytical balance to determine the weight difference [55, 56].

Thickness

A digital vernier calliper can be utilised to measure thickness at multiple points on the MDF F1-F4. Ensuring uniform thickness is critical, as it directly impacts the dosage accuracy of the MDF strips [57, 58].

Folding endurance

Folding endurance of F1-F4 is found by folding the strip in the same spot over and over until it breaks. The quantity of folds that the MDF can withstand without showing signs of cracking is used to calculate the folding endurance value [59, 60].

Tensile strength

Tensile strength (TS) of F1-F4 was determined on a texture analyser. A film strip (usually 2×5 cm2) was held between two jaws and pulled at a constant rate until it fractured [61,62]. The formula was used to calculate the TS:

$$TS = \frac{\text{Force at break (N)}}{\text{Cross-sectional area of the film (mm)}} \ldots. (1)$$

Percentage elongation

The lengthening of a film before breaking was recorded during the tensile strength test. The Percentage Elongation for F1-F4 was assessed [63, 64]. Percentage elongation was calculated as:

$$\% \text{ elongation} = \frac{\text{Increase in length}}{\text{original length}} \times 100 \ldots. (2)$$

Disintegration time

In a petri dish, 10 ml of simulated saliva fluid (pH 6.8) was added to a film strip (2 x 2 cm^2), which was kept at 37±0.5 °C. The disintegration time was defined as the amount of time it took for the film to fully dissolve [65, 66]. The Disintegration time of F1-F4 was measured.

Content uniformity

Three uniform-sized samples of film F1-F4 were cut from varying regions of the film. One sample from each region was dissolved in an appropriate solvent, sonicated, filtered, and a UV Spectrophotometer was utilized to analyze each sample at 240 nm. Comparisons of each sample's drug content were made to determine uniformity [67, 68].

Drug content

A known 2×2 cm2 area of the film F1-F4 was dissolved in 10 ml of a suitable solvent. After filtering the solution, the drug concentration was measured using spectrophotometry at 240 nm. A percentage of the theoretical drug loading was used to represent the drug content [69, 70].

***In vitro* drug release studies of MDFs (F1-F4)**

The drug release of SMEDDS integrated MDF (F1-F3) and pure NIFD loaded film (F4) was analysed by using Franz diffusion cells with 12 ml capacity receptor chambers to evaluate the release profiles of API from SMEDDS-MDF and assess the influence of self-microemulsifying properties on drug diffusion. The literature suggested the use of Franz diffusion cells for *in vitro* drug release testing from MDFs, because the films rapidly hydrate and fragment under paddle agitation in the USP II dissolution apparatus, making it unsuitable for studying formulation-controlled release. The Franz cell maintains a fixed diffusion area, prevents film breakup, and better represents early buccal diffusion behaviour. A cellulose acetate membrane was employed as an inert barrier to maintain film structure, and sink conditions were maintained through medium replacement. A pH 6.8 PB solution was added to the chambers while stirring magnetically, and MDF fragments (2×2 cm^2) were placed in the donor chambers. The collected samples were diluted and examined using a UV spectrophotometer at 240 nm [71–73].

The *in vitro* drug release profiles obtained for each MDF formulation were analyzed using the following kinetics,

1. Zero-order kinetic model [Cumulative % drug released versus time]

2. First-order kinetic model [Log cumulative % drug remaining versus time]

3. Higuchi plot [Cumulative % drug release versus square root of time]

4. Koresmeyer-Peppas model [Log cumulative % drug release versus log T]

Drug release study of SMEDDS integrated films and pure NIFD film

An *in vitro* drug release study was performed between the SMEDDS-integrated film (F1) and the pure nifedipine film (F4) using the same Franz diffusion cell setup described earlier. Both films, equivalent to 10 mg of nifedipine, were tested under identical conditions to evaluate differences in their drug release behaviour. Samples were collected at predetermined intervals and analysed spectrophotometrically at 240 nm, and the release profiles of the two formulations [74].

RESULTS AND DISCUSSION

Construction of pseudo-ternary phase diagram

To ascertain the extent of microemulsion regions at room temperature, pseudo-ternary phase diagrams were constructed by using the water titration method. The formulations were diluted with filtered water and analyzed to identify the optimal Smix and oil ratio within the SMEDDS formulation. The pseudo-ternary phase diagrams were constructed to identify the self-microemulsifying region within the oil-Smix-water system. Each vertex represents 100% of one component, with gridlines showing 10% intervals. The Smix 1:2 (Tween 80: Span 80) system exhibited a broader and more stable microemulsion region (≈42–70%) than Smix 1:1 (≈30–55%), indicating superior emulsification due to higher co-surfactant content. Therefore, Smix 1:2 was selected for further optimisation using the Box–Behnken Design, with the composition range defined from the ternary diagram forming the basis for DoE formulation studies. The shaded area in the pseudo-ternary diagram illustrates the microemulsion region in which oil-in-water (o/w) self-microemulsification occurs (fig. 2). The emulsification efficiency increased with the size of the microemulsion region, with larger regions resulting in greater efficiency; the boundaries in the fig. were selected based on weight ratios of oil-water-Smix [75].

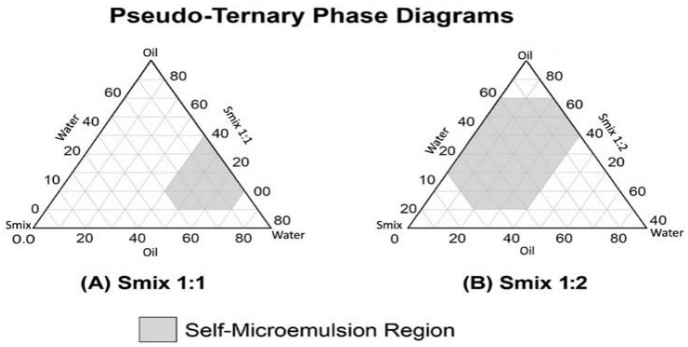

Fig. 2: Pseudo-ternary phase diagram representing the microemulsion region for various ratios of oil, water, surfactant, and co-surfactant (Smix) 1:1 and 1:2

Optimisation of SMEDDS formulation using BBD

The study involved a thorough evaluation of all dependent variables and conducted both numerical and graphical optimizations. The numerical optimization aimed to maximize the dependent variables while maintaining the independent variables within a specified range. The lower and upper limits of the independent variables were established, while the dependent variables' upper and lower bounds were determined from the responses [76].

The design proposed 13 possible runs based on the combinations of input variables. After conducting all the experimental runs and inputting the corresponding responses into the design software, an analysis was performed, resulting in the optimized formulation design. All 13 experiments were carried out according to the specified procedure, and the resulting data were recorded and entered into the design for further analysis**.** The DoE-generated design is given in table 2.

Table 2: Formulation composition of NIFD-SMEDDS formulation factors, FS1-FS13 runs, and corresponding responses, droplet size, and transmittance

Formulation code	Std	Run	Independent variables			Dependent variables	
			Factor 1 A: Castor oil (mg)	Factor 2 B: Tween 80 (mg)	Factor 3 C: Span 80 (mg)	Response 1 (Y1) Droplet size (nm)	Response 2 (Y2) Transmittance (%)
FS1	10	1	32.9	347.8	23.5	210	97.8
FS2	1	2	108.1	347.8	23.5	265	87.9
FS3	4	3	132.9	441.8	23.5	267	98.9
FS4	7	4	108.1	441.8	23.5	286	97.8
FS5	2	5	32.9	394.8	9.4	198	94.3
FS6	6	6	108.1	394.8	9.4	278	86.7
FS7	8	7	32.9	394.8	37.6	199	99.7
FS8	13	8	108.1	394.8	37.6	276	97.2
FS9	9	9	70.5	347.8	9.4	223	82.3
FS10	11	10	70.5	441.8	9.4	233	87.6
FS11	5	11	70.5	347.8	37.6	243	85.3
FS12	12	12	70.5	441.8	37.6	254	96.3
FS13	3	13	70.5	394.8	23.5	221	91.3

The response (Y1)

BBD generally employs a quadratic model to capture curvature and interaction effects. Statistical analysis of the droplet size data indicated that none of the quadratic (A^2, B^2, C^2) or interaction (AB, AC, BC) terms were significant ($p>0.05$) based on ANOVA. Therefore, a reduced linear model was adopted as the best fit for droplet size. The simplified regression equation obtained was:

Droplet size (nm) **(**Y1) =+236.99+31.94 (A)+1.87 (B)+5.32 (C)

The model exhibited good correlation (R^2 = 0.855, F = 17.89, p = 0.0004), confirming its adequacy. Among the factors, castor oil concentration (A) had the most significant effect ($p<0.0001$), indicating that increasing oil proportion led to a proportional rise in droplet size, whereas Tween 80 (B) and Span 80 (C) exerted minor influences. The impact of A, B, and C on Y_1 had been represented on a 3D response surface plot in fig. 3 (A) and table 3.

The response (Y2)

For the response variable % transmittance (Y_2), an initial quadratic model including all main, interaction, and squared terms (A, B, C, AB, AC, BC, A^2, B^2, C^2) was fitted. Based on ANOVA, the interaction terms (AB, AC, BC) and the quadratic terms B^2 and C^2 were found to be statistically nonsignificant ($p>0.05$) and were therefore excluded from the final model. The reduced quadratic equation obtained after model refinement was:

Transmittance (%) (Y2) =+89.66-3.34A+3.43B+3.67C+5.25A2

The model exhibited good overall fit (F = 11.76, p = 0.0020; R^2 = 0.856), confirming its adequacy for predicting optical clarity. The positive coefficients of Tween 80 (B) and Span 80 (C) indicate that increasing surfactant and co-surfactant levels improved transmittance, whereas higher oil concentration (A) slightly decreased it. The significant positive A^2 term suggests a mild curvature effect for oil concentration on transmittance, reflecting a balance between emulsification efficiency and droplet size. The impact of A, B, and C on Y2 was represented on a 3D response surface plot in fig. 3(B). The ANOVA results of the design are given in table 3.

DoE optimized formulation

Three optimized SMEDDS formulations, FS14, FS15, and FS16, were prepared to obtain the minimum droplet size and maximum transmittance. The optimum levels of independent variables (A), (B), and (C) were obtained from desirability function analysis. The optimized three formulations had droplet sizes<210 nm and transmittance (>93%), which indicated that emulsification and stability in these emulsions were good. The close correlations of the actual and predicted values proved the accuracy of the model used for optimization. Overlay plots are given in fig. 4. The outcomes support the effective use of the BBD employed in formulating an effective SMEDDS system for NIFD. The optimized formulations were obtained by keeping the span 80 at the lowest quantity. Good correlation between actual and predicted values by design to the chosen responses, droplet size (Y1), and transmittance (Y2) in optimized SMEDDS formulations (FS14–FS16) indicates the best fitting of the chosen design for the optimization. Results are given in table 4.

Characterization of SMEDDS

Droplet size, PDI, Zeta potential, cloud point, and dispersibility of optimised SMEDDS

Recent advancements in SMEDDS have demonstrated promising strategies for enhancing the solubility of BCS Class II drugs such as NIFD. For example, Bindhani *et al.* (2020) formulated NIFD-loaded SMEDDS, achieving improved solubility but with no integration into fast-dissolving dosage forms. Similarly, Jannin *et al.* (2015) focused on lipid-based formulations but did not address patient compliance aspects such as portability and ease of use. Droplet size ranges from 198-286 nm (optimized batches show 196±5-201±**3** nm). The Droplet size of FS14 is given in fig. 5. The optimized SMEDDS showed PDI values of 0.534–0.608, indicating a relatively polydisperse system compared to the ideal PDI 0.3 for stable nanoemulsions. Such a broad size distribution suggests possible droplet coalescence or phase instability, which may affect reproducibility and absorption consistency. Future optimization should aim to reduce PDI for improved uniformity and stability. The zeta potential values (-15 to-21 mV) indicate moderate electrostatic stabilization; however, the presence of non-ionic surfactants (Tween 80 and Span 80) provides additional steric stabilization, contributing to overall system stability. No visible creaming or phase separation was observed over three months. The cloud points (65-75 °C) confirm thermal stability, ensuring that storage at room temperature or use at 37 °C remains safely below the surfactant

dehydration threshold. The zeta potential of FS14 is given in fig. 6. Cloud point values between 65±2 and 75±2 °C ensured the thermal stability of SMEDDS at physiological conditions. Dispersibility studies showed fast emulsification with Grade A and B ratings, ensuring effective self-emulsification behaviour [77]. The solubility ranges from 15.2±2-71.5±2 µg/ml. Results are given in table 5.

Table 3: Summary of ANOVA study showing the significant effect of chosen factors of formulation on droplet size (Y1) – linear model and transmittance (Y2) – Quadratic model

Response (Y1) Droplet size (nm)						
Source	**Sum of squares**	**df**	**Mean square**	**F-value**	**p-value**	**Source**
Model (linear)	9741.96	3	3247.32	17.89	0.0004	significant
A-oil	8316.84	1	8316.84	45.83	<0.0001	
B-surfactant	25.23	1	25.23	0.1390	0.7179	
C-co-surfactant	200.00	1	200.00	1.10	0.3212	
Residual	1633.27	9	181.47			
Cor Total	11375.23	12				
Response (Y2) Transmittance (%)						
Source	Sum of squares	df	Mean square	F-value	p-value	
Model (quadratic)	363.12	4	90.78	11.76	0.0020	significant
A-oil	78.53	1	78.53	10.18	0.0128	
B-surfactant	84.01	1	84.01	10.89	0.0109	
C-co-surfactant	95.22	1	95.22	12.34	0.0079	
A^2	153.56	1	153.56	19.90	0.0021	
Residual	61.73	8	7.72			
Cor Total	424.85	12				

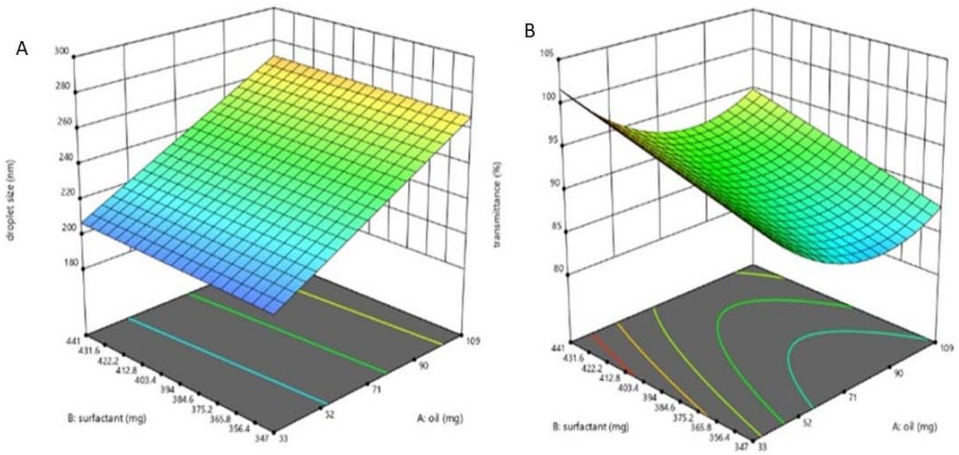

Fig. 3: 3D response surface plots illustrating the effect of oil and surfactant concentration on droplet size (nm) (A) and transmittance (%) (B) of SMEDDS formulations

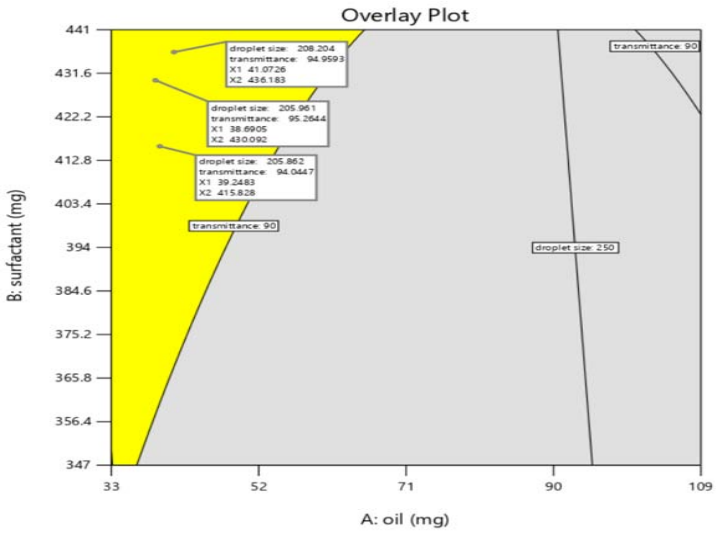

Fig. 4: Overlay plot illustrating the optimized region for SMEDDS formulation based on droplet size (nm) and transmittance (%), highlighting the influence of oil and surfactant concentrations

Table 4: Actual versus predicted values of responses, droplet size (Y1), and transmittance (Y2) in optimized SMEDDS formulations (FS14–FS16)

Optimized batch	Independent variable			Dependent variable			
	A (mg)	B (mg)	C (mg)	Actual values (Mean±sd)*		Predicted values	
				Y1 droplet size (nm)	Y2 transmittance (%)	Y1 droplet size (nm)	Y2 transmittance (%)
FS14	39.24	415.82	9.4	198±4	90±0.3	205.86	94.04
FS15	38.69	430.09	9.4	196±5	92±0.4	205.96	95.26
FS16	41.07	436.18	9.4	201±3	89±0.5	208.20	94.95

Results are expressed in mean±sd*(n = 3).

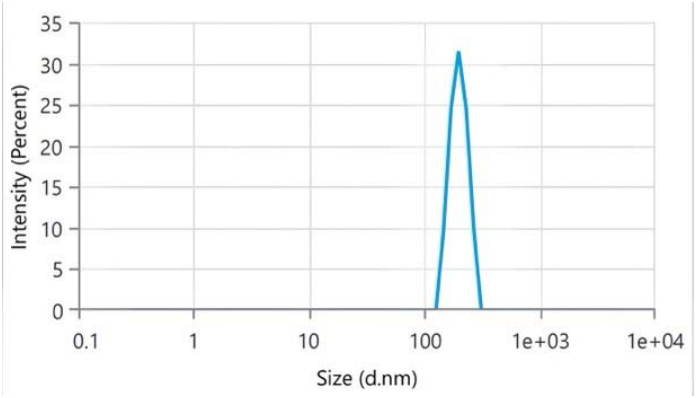

Fig. 5: Droplet size distribution of optimised SMEDDS formulation FS14, indicating nanoscale droplet size

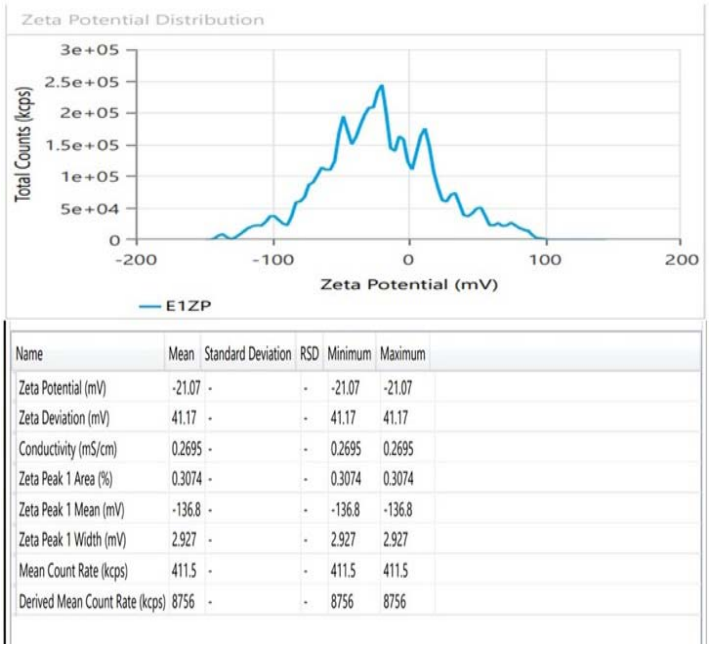

Name	Mean	Standard Deviation	RSD	Minimum	Maximum
Zeta Potential (mV)	-21.07	-	-	-21.07	-21.07
Zeta Deviation (mV)	41.17	-	-	41.17	41.17
Conductivity (mS/cm)	0.2695	-	-	0.2695	0.2695
Zeta Peak 1 Area (%)	0.3074	-	-	0.3074	0.3074
Zeta Peak 1 Mean (mV)	-136.8	-	-	-136.8	-136.8
Zeta Peak 1 Width (mV)	2.927	-	-	2.927	2.927
Mean Count Rate (kcps)	411.5	-	-	411.5	411.5
Derived Mean Count Rate (kcps)	8756	-	-	8756	8756

Fig. 6: The zeta potential of the optimized SMEDDS formulation FS14 confirmed its colloidal stability

Table 5: Physicochemical properties, PDI, Zeta potential, Cloud point temperature, Dispersibility grade, and solubility of FS14–FS16 (optimised SMEDDS) and pure NIFD drug

Formulation	PDI (Mean±sd)*	Zeta potential (mV) (Mean±sd)*	Cloud point (c)(Mean±sd)*	Dispersibility		Solubility (µg/ml) (Mean±sd)*
				Time (s) (Mean±sd)*	Grade	
FS14	0.534±0.01	-20.27±2.5	75±2	20±2	A	71.5±2
FS15	0.566±0.03	-17.86±1.7	68±3	50±3	B	67.8±3
FS16	0.608±0.02	-15.66±1.2	65±2	75±2	B	58.6±2
Pure NIFD.	-	-	-	-		20.2±2

Results are expressed in mean±sd (n = 3).

Surface morphology analysis of pure NIFD integrated MDF (F4) with SMEDDS integrated MDF (F1)

SEM images of Plain film F4 (NIFD loaded MDF) (A) and F1(NIFD-SMEDDS integrated MDF) (B) are given in fig. 7. This morphological change, crucial for enhancing solubility and dissolution, aligns with findings from Sharma *et al.* (2012), who emphasised surface morphology's role in drug release kinetics in solidified SMEDDS and integrated MDF revealed the presence of SMEDDS droplets without any signs of drug crystallisation, and film containing pure NIFD is a plain with a smooth surface. At the magnification used, the SMEDDS-loaded films (F1) exhibited a more heterogeneous and uneven surface texture compared to the smooth morphology of the pure NIFD-loaded film (F4), suggesting dispersion of the lipidic phase within the polymer matrix.

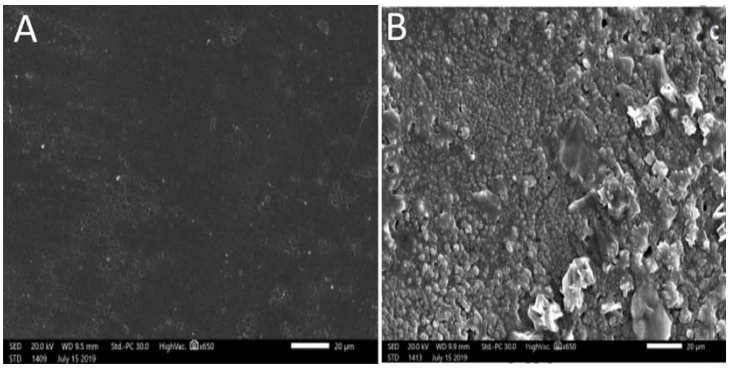

Fig. 7: SEM images illustrating the surface morphology of (A) plain film, F4, and (B) SMEDDS-embedded MDF, F1, emphasizing the modifications resulting from SMEDDS incorporation

Fourier transform infrared (FT-IR) spectroscopy.

The spectra of individual components, the SMEDDS mixture, and the final formulation were compared to detect any potential interactions or structural modifications. The pure NIFD spectrum exhibited characteristic peaks at 1116 cm^{-1} (C-O stretching), 1353 cm^{-1} (N-O stretching), 1531 cm^{-1} (C=C stretching), and 1702 cm^{-1} (C=O stretching), confirming the presence of its functional groups. The excipients, including PVP, HPMC, PEG, castor oil, Span 20, and Tween 80, displayed their characteristic peaks, such as 1650 cm^{-1} for PVP (C=O stretching), 1050 cm^{-1} for HPMC (C-O stretching), and 1735 cm^{-1} for castor oil (C=O stretching). The SMEDDS mixture showed minor peak shifts and broadening, indicating physical interactions but no significant chemical modifications. In the final formulation, the retention of NIFD's key peaks, particularly 1702 cm^{-1} (C=O stretching), suggests that the drug remained intact. The presence of broad peaks around 3400–3421 cm^{-1} (O-H stretching) suggests hydrogen bonding between the polymer and excipients, potentially enhancing drug stability and solubility. Overall, the FTIR analysis confirms that there are no significant chemical interactions, ensuring the stability and compatibility of the SMEDDS-based film for pharmaceutical applications [78–80]. The FTIR spectra are given in fig. 8. This is consistent with reports by Ghosh *et al.* (2011) and Lou *et al.* (2023), who used FTIR to confirm molecular-level compatibility in similar systems.

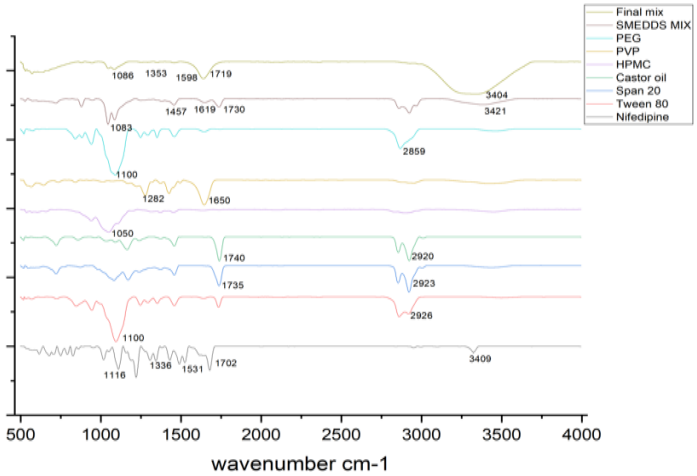

Fig. 8: FTIR spectra comparing pure NIFD, individual excipients, SMEDDS mixture, and final MDF formulation to assess compatibility

Evaluation of optimized SMEDDS integrated MDF

The F1-F4 with optimized formulation had appropriate physicochemical and mechanical characteristics. The pH ranged from 5.41±0.06 to 6.85±0.03, reflecting compatibility with the oral mucosa. Weight variation was low, ranging from 98.4±1.2 to 102.1±0.9 mg, and thus maintaining uniformity in dosage. The thickness of the film ranged from 0.11±0.005 to 0.15±0.004 mm, reflecting uniformity in casting. Folding endurance was between 21±2 and 54±4 folds, which showed good elasticity and resistance to rupture. Mechanical strength tests indicated tensile strength values of between 4.8±0.2 to 5.2±0.3 N/mm^2, and percentage elongation of between 13.9±0.6 to 15.2±0.4 %, showing the films were elastic but strong. Disintegration time was fast, ranging from 48±2 to 60±2 sec, suitable for rapid onset of action in buccal delivery [81, 82]. Uniformity of content was uniform across all samples between 80.5±0.5 % w/w and 99.2±0.4 % w/w, and drug content varied between 87.04±1.0 % w/w and 95.08±0.6 % w/w, validating successful drug loading and homogeneity. Results are given in table 6.

Table 6: Evaluation of physicochemical properties, content uniformity, and disintegration time of SMEDDS-loaded MDFs (F1–F3) and pure NIFD-loaded MDF (F4)

S. No.	Parameter	F1 (Mean±sd)*	F2 (Mean±sd)*	F3 (Mean±sd)*	F4 (Mean±sd)*
1.	pH	6.10±0.05	6.08±0.04	5.41±0.06	6.85±0.03
2.	Weight Variation (mg)	98.4±1.2	102.1±0.9	100.6±1.4	99.2±1.1
3.	Thickness (mm)	0.12±0.05	0.15±0.004	0.13±0.006	0.11±0.005
4.	Folding Endurance (folds)	54±4	43±3	48±5	21±2
5.	Tensile Strength (N/mm^2)	4.8±0.2	5.2±0.3	4.9±0.2	5.1±0.3
6.	% Elongation	14.5±0.5	15.2±0.4	13.9±0.6	14.8±0.3
7.	Disintegration Time (sec)	48±2	52±3	54±2	60±2
8.	Content Uniformity (%) w/w	98.7±0.6	99.2±0.4	97.9±0.7	80.5±0.5
9.	Drug Content (%) w/w	95.08±0.6	92.86±0.8	90.30±0.5	87.04±1.0

Results are expressed in mean±sd (n = 3).

Drug release and kinetic studies

F1 demonstrated a superior release profile compared to the other formulations. Hence, F1 can be considered the most optimal among the four formulations tested. The drug release profiles of F1-F4 are given in fig. 9. The *in vitro* release kinetics of NIFD-SMEDDS-loaded mouth dissolving film were evaluated using various mathematical models, including Zero Order, First Order, Higuchi, and Korsmeyer-Peppas [83]. It shows greater correlation for first-order ($R^2 \approx 0.979$) and Higuchi kinetic ($R^2 \approx 0.988$) models, since nifedipine is solubilized within SMEDDS droplets embedded in a rapidly dissolving polymer matrix, the drug release is more likely governed by film hydration, matrix erosion, and diffusion of solubilized drug, table 7 describes the release kinetics.

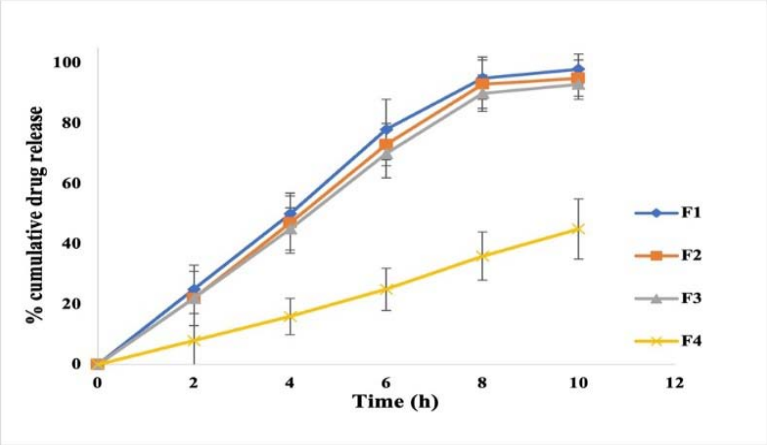

Fig. 9: Comparative *in vitro* drug release profiles of NIFD from SMEDDS-MDFs (F1–F3), plain NIFD-MDF (F4), highlighting enhanced drug diffusion from the SMEDDS integrated MDF formulations

Table 7: Regression coefficients (R^2) of *in vitro* drug release profiles of SMEDDS integrated MDF (F1) using different kinetic models

Release kinetic model	Formulation-F1 (R^2)
Zero Order	0.9561
First Order	0.9789
Higuchi	0.9875
Kors Meyer – Peppa's	0.9067

NIFD release from pure NIFD MDFs and NIFD-SMEDDS integrated MDFs

The dissolution profiles clearly demonstrated that formulation F1 (SMEDDS-loaded MDF) exhibited a markedly faster and more complete drug release than F4 (pure nifedipine film). Within the first 10 min, F1 achieved more than 70% cumulative drug release, whereas F4 released less than 40% in the same period. Complete drug release from F1 occurred within 45 min, while F4 reached only about 65-70% by the end of the study. This increased drug release can be attributed to the pre-solubilised state of nifedipine within the SMEDDS droplets and the rapid hydration and erosion of the polymeric film, which together promote efficient drug diffusion into the dissolution medium. In contrast, the pure drug film exhibited slower dissolution due to nifedipine's poor aqueous solubility and limited wetting. Thus, the SMEDDS-integrated film significantly improved the drug release, confirming the formulation's superior dissolution performance.

CONCLUSION

The current research successfully developed and optimized NIFD-loaded SMEDDS to develop MDF through BBD. The best SMEDDS formulation was acceptable with respect to droplet size, transmittance, zeta potential, and dispersibility. Such features indicate satisfactory emulsification and stability. The SMEDDS-integrated MDFs have acceptable physico-mechanical properties, including consistent weight and thickness, high folding endurance, tensile strength, and shorter disintegration time. Characterisation using FTIR and SEM confirmed the compatibility of excipients and the uniform dispersion of SMEDDS in the MDF. The *in vitro* drug diffusion studies revealed that SMEDDS-integrated MDF showed increased drug diffusion profiles, and the release profiles were best fitted to the Higuchi and the First-order model. Therefore, this study provides evidence that SMEDDS-MDFs could be a patient-friendly alternative to enhance the oral bioavailability of BCS-III drugs such as NIFD. Although the present investigation did not include stability

testing of the final films, such evaluation will be conducted in future studies to confirm the storage stability, mechanical robustness, and shelf-life of the optimized formulation.

FUNDING

Nil

AUTHORS CONTRIBUTIONS

[Sowmya C*]-ideation and execution of the project, drafted the manuscript; [Dhanush R]-literature search, optimisation of SMEDDS formulation; [Preethika S]-Formulation and characterisation of SMEDDS and SMEDDS integrated MDFs; [Sujatha K]-compilation of results and finalisation of the manuscript.

CONFLICT OF INTERESTS

Declared none

REFERENCES

1. Alqahtani MS, Kazi M, Alsenaidy MA, Ahmad MZ. Advances in oral drug delivery. Front Pharmacol. 2021 Feb;12:618411. doi: 10.3389/fphar.2021.618411, PMID 33679401.
2. Gupta H, Bhandari D, Sharma A. Recent trends in oral drug delivery: a review. Recent Pat Drug Deliv Formul. 2009;3(2):162-73. doi: 10.2174/187221109788452267, PMID 19519576.
3. Lou J, Duan H, Qin Q, Teng Z, Gan F, Zhou X. Advances in oral drug delivery systems: challenges and opportunities. Pharmaceutics. 2023;15(2):484. doi: 10.3390/pharmaceutics15020484, PMID 36839807.
4. Sastry SV, Nyshadham JR, Fix JA. Recent technological advances in oral drug delivery a review. Pharm Sci Technol Today. 2000;3(4):138-45. doi: 10.1016/S1461-5347(00)00247-9, PMID 10754543.
5. Haware RV, Vinjamuri BP, Gavireddi M, Dave VS, Gupta D, Chougule MB. Physical properties and solubility studies of nifedipine-PEG 1450/HPMCAS-HF solid dispersions. Pharm Dev Technol. 2019;24(5):550-9. doi: 10.1080/10837450.2018.1519573, PMID 30175691.
6. Hecq J, Nollevaux G, Deleers M, Fanara D, Vranckx H, Peulen O. Nifedipine nanocrystals: pharmacokinetic evaluation in the rat and permeability studies in Caco-2/HT29-5M21 (co)-cultures. J Drug Deliv Sci Technol. 2006;16(6):437-42. doi: 10.1016/S1773-2247(06)50084-X.
7. Bindhani S, Mohapatra U, Mohapatra S, Kar RK. Enhancement of solubility and dissolution rate of poorly soluble drug nifedipine by solid sedds. Int J Drug Deliv Technol. 2020;10(1):9-15. doi: 10.25258/ijddt.10.1.3.
8. Jannin V, Chevrier S, Michenaud M, Dumont C, Belotti S, Chavant Y. Development of self-emulsifying lipid formulations of BCS class II drugs with low to medium lipophilicity. Int J Pharm. 2015;495(1):385-92. doi: 10.1016/j.ijpharm.2015.09.009, PMID 26364710.
9. Rahman MA, Hussain A, Hussain MS, Mirza MA, Iqbal Z. Role of excipients in successful development of self-emulsifying/microemulsifying drug delivery system (SEDDS/SMEDDS). Drug Dev Ind Pharm. 2013;39(1):1-19. doi: 10.3109/03639045.2012.660949, PMID 22372916.
10. Maurya SD, Arya RK, Rajpal G, Dhakar RC. Self-micro emulsifying drug delivery systems (Smedds): a review on physico-chemical and biopharmaceutical aspects. J Drug Deliv Ther. 2017;7(3):55-6. doi: 10.22270/jddt.v7i3.1453.
11. Sharma V, Singh J, Gill B, Harikumar SL. Smedds: a novel approach for lipophilic drugs. IJPSR. 2012;3(8):8. doi: 10.13040/IJPSR.0975-8232.3(8).2441-50.
12. Gahlawat N, Verma R, Kaushik D. Recent developments in self-microemulsifying drug delivery system: an overview. Asian J Pharm. 2019;13(2):59. doi: 10.22377/ajp.v13i02.3101.
13. Rathod S, Phansekar M, Bhagwan A, Surve G. A review on mouth dissolving tablets. Indian Drugs. 2013;50(11):5-14. doi: 10.53879/id.50.11.p0005.
14. Thakur N, Bansal M, Sharma N, Yadav G, Khare P. Overview a novel approach of fast dissolving films and their patients. Adv Biol Res (Rennes). 2013;7(2):50-8. doi: 10.5829/idosi.abr.2013.7.2.72134.
15. Ghodake PP, Karande KM, Osmani A, Bhosale RR, Harkare BR, Kale BB. Mouth dissolving films: innovative vehicle for oral drug delivery. Int J Pharm Res Rev. 2013;2(10):41-7.
16. Jain P, Gupta A, Darwhekar G. An detailed overview on mouth dissolving film. J Drug Deliv Ther. 2023;13(7):172-6. doi: 10.22270/jddt.v13i7.6121.
17. Xie S, Zhao B. Phase equilibrium studies of nonferrous smelting slags: a review. Metals. 2024;14(3):278. doi: 10.3390/met14030278.
18. Ma YJ, Yuan XZ, Xin-Peng HW, Hou-Wang HJ, Huang HL, Shan-Bao ZH. The pseudo-ternary phase diagrams and properties of anionic-nonionic mixed surfactant reverse micellar systems. J Mol Liq. 2015;203:181-6. doi: 10.1016/j.molliq.2014.12.043.
19. Popovic Milenkovic MT, Tomovic MT, Brankovic SR, Ljujic BT, Jankovic SM. Antioxidant and anxiolytic activities of Crataegus nigra Wald. Et kit. Berries. Acta Pol Pharm. 2014;71(2):279-85. PMID 25272648.
20. Gunarto C, Ju YH, Putro JN, Tran-Nguyen PL, Soetaredjo FE, Santoso SP. Effect of a nonionic surfactant on the pseudoternary phase diagram and stability of microemulsion. J Chem Eng Data. 2020;65(8):4024-33. doi: 10.1021/acs.jced.0c00341.
21. Xue X, Cao M, Ren L, Qian Y, Chen G. Preparation and optimization of Rivaroxaban by self-nanoemulsifying drug delivery system (SNEDDS) for enhanced oral bioavailability and no food effect. AAPS PharmSciTech. 2018;19(4):1847-59. doi: 10.1208/s12249-018-0991-6, PMID 29637496.
22. Singh AK, Chaurasiya A, Singh M, Upadhyay SC, Mukherjee R, Khar RK. Exemestane loaded self-microemulsifying drug delivery system (SMEDDS): development and optimization. AAPS PharmSciTech. 2008;9(2):628-34. doi: 10.1208/s12249-008-9080-6, PMID 18473177.
23. Akula S, Gurram AK, Devireddy SR, Deshpande PB. Evaluation of surfactant effect on self-micro emulsifying drug delivery system (SMEDDS) of lercanidipine hydrochloride: formulation and evaluation. J Pharm Innov. 2015 Dec 16;10(4):374-87. doi: 10.1007/s12247-015-9233-6.
24. Lee DW, Marasini N, Poudel BK, Kim JH, Cho HJ, Moon BK. Application of box-behnken design in the preparation and optimization of fenofibrate-loaded self-microemulsifying drug delivery system (SMEDDS). J Microencapsul. 2014;31(1):31-40. doi: 10.3109/02652048.2013.805837, PMID 23834315.
25. Shen H, Zhong M. Preparation and evaluation of self-microemulsifying drug delivery systems (SMEDDS) containing atorvastatin. J Pharm Pharmacol. 2006;58(9):1183-91. doi: 10.1211/jpp.58.9.0004, PMID 16945176.
26. Pramanik S, Thakkar H. Development of solid self-microemulsifying system of tizanidine hydrochloride for oral bioavailability enhancement: *in vitro* and *in vivo* evaluation. AAPS PharmSciTech. 2020;21(5):182. doi: 10.1208/s12249-020-01734-9, PMID 32613377.
27. Wei L, Sun P, Nie S, Pan W. Preparation and evaluation of SEDDS and SMEDDS containing carvedilol. Drug Dev Ind Pharm. 2005;31(8):785-94. doi: 10.1080/03639040500216428, PMID 16221613.
28. Varshosaz J, Dehghan Z. Development and characterization of buccoadhesive nifedipine tablets. Eur J Pharm Biopharm. 2002;54(2):135-41. doi: 10.1016/S0939-6411(02)00078-4, PMID 12191683.
29. Yan G, Li H, Zhang R, Ding D. Preparation and evaluation of a sustained-release formulation of nifedipine HPMC tablets. Drug Dev Ind Pharm. 2000;26(6):681-6. doi: 10.1081/DDC-100101284, PMID 10826117.
30. Joshi P, Patel H, Patel V, Panchal R. Formulation development and evaluation of mouth dissolving film of domperidone. J Pharm Bioallied Sci. 2012;4(Suppl 1):S108-9. doi: 10.4103/0975-7406.94159, PMID 23066181.
31. Mud D, Gunashekar SA, Singh Mangla N, Ajay K. Formulation and evaluation of mouth dissolving film containing kulkarni parthasarathi keshavarao. Int Res J Pharm. 2011;2(3):273-8. doi: 10.7897/2230-8407.
32. Upret K, Kumar L, Anand SP, Chawla V. Formulation and evaluation of mouth dissolving films of paracetamol. Int J Pharm Pharm Sci. 2014;6(5):200-2.
33. Pawar SV, Junagade MS. Formulation and evaluation of mouth dissolving film of risperidone. Int J PharmTech Res. 2015;8(6):218-30.

34. Bachhav YG, Patravale VB. SMEDDS of glyburide: formulation *in vitro* evaluation and stability studies. AAPS PharmSciTech. 2009;10(2):482-7. doi: 10.1208/s12249-009-9234-1, PMID 19381824.
35. Borhade V, Nair H, Hegde D. Design and evaluation of self-microemulsifying drug delivery system (SMEDDS) of tacrolimus. AAPS PharmSciTech. 2008;9(1):13-21. doi: 10.1208/s12249-007-9014-8, PMID 18446456.
36. Dixit AR, Rajput SJ, Patel SG. Preparation and bioavailability assessment of SMEDDS containing valsartan. AAPS PharmSciTech. 2010;11(1):314-21. doi: 10.1208/s12249-010-9385-0, PMID 20182825.
37. Algahtani MS, Ahmad MZ, Ahmad J. Investigation of factors influencing formation of nanoemulsion by spontaneous emulsification: impact on droplet size polydispersity index and stability. Bioengineering (Basel). 2022;9(8):384. doi: 10.3390/bioengineering9080384, PMID 36004909.
38. Shah R, Eldridge D, Palombo E, Harding I. Optimisation and stability assessment of solid lipid nanoparticles using particle size and zeta potential. J Phys Sci. 2014;25(1):59-75.
39. Lee JH, Lee GW. Formulation approaches for improving the dissolution behavior and bioavailability of Tolvaptan using SMEDDS. Pharmaceutics. 2022;14(2):415. doi: 10.3390/pharmaceutics14020415, PMID 35214147.
40. Kristiani M, Martien R, Martien R, Ismail H, Yuswanto A. Cytotoxic activity of acidic ribosome inactivating proteins Mirabilis jalapa L. Int J Pharm Pharm Sci. 2017 August 1;9(8):69. doi: 10.22159/ijpps.2017v9i8.18171.
41. Singh AK, Chaurasiya A, Awasthi A, Mishra G, Asati D, Khar RK. Oral bioavailability enhancement of exemestane from self-microemulsifying drug delivery system (SMEDDS). AAPS PharmSciTech. 2009;10(3):906-16. doi: 10.1208/s12249-009-9281-7, PMID 19609837.
42. Akula S, Gurram AK, Devireddy SR, Deshpande PB. Evaluation of surfactant effect on self micro emulsifying drug delivery system (SMEDDS) of lercanidipine hydrochloride: formulation and evaluation. J Pharm Innov. 2015;10(4):374-87. doi: 10.1007/s12247-015-9233-6.
43. Jankovic J, Djekic L, Dobricic V, Primorac M. Evaluation of critical formulation parameters in design and differentiation of self-microemulsifying drug delivery systems (SMEDDSS) for oral delivery of aciclovir. Int J Pharm. 2016;497(1-2):301-11. doi: 10.1016/j.ijpharm.2015.11.011, PMID 26611669.
44. Dhaval M, Panjwani M, Parmar R, Soniwala MM, Dudhat K, Chavda J. Application of simple lattice design and desirability function for formulating and optimizing SMEDDS of clofazimine. J Pharm Innov. 2021;16(3):504-15. doi: 10.1007/s12247-020-09468-8.
45. Rajesh SY, Singh SK, Pandey NK, Sharma P, Bawa P, Kumar B. Impact of various solid carriers and spray drying on pre/post compression properties of solid SNEDDS loaded with glimepiride: *in vitro*-ex vivo evaluation and cytotoxicity assessment. Drug Dev Ind Pharm. 2018;44(7):1056-69. doi: 10.1080/03639045.2018.1431656, PMID 29360412.
46. Thi TD, Van Speybroeck M, Barillaro V, Martens J, Annaert P, Augustijns P. Formulate-ability of ten compounds with different physicochemical profiles in SMEDDS. Eur J Pharm Sci. 2009;38(5):479-88. doi: 10.1016/j.ejps.2009.09.012, PMID 19782131.
47. Kim DS, Cho JH, Park JH, Kim JS, Song ES, Kwon J. Self-microemulsifying drug delivery system (SMEDDS) for improved oral delivery and photostability of methotrexate. Int J Nanomedicine. 2019;14:4949-60. doi: 10.2147/IJN.S211014, PMID 31308665.
48. Sun C, Gui Y, Hu R, Chen J, Wang B, Guo Y. Preparation and pharmacokinetics evaluation of solid self-microemulsifying drug delivery system (S-SMEDDS) of osthole. AAPS PharmSciTech. 2018;19(5):2301-10. doi: 10.1208/s12249-018-1067-3, PMID 29845504.
49. Madagul JK, Parakh DR, Kumar RS, Abhang RR. Formulation and evaluation of solid self-microemulsifying drug delivery system of chlorthalidone by spray drying technology. Drying Technol. 2017;35(12):1433-49. doi: 10.1080/07373937.2016.1201833.
50. Patel PV, Patel HK, Panchal SS, Mehta TA. Self-micro-emulsifying drug delivery system of tacrolimus: formulation *in vitro* evaluation and stability studies. Int J Pharm Investig. 2013;3(2):95-104. doi: 10.4103/2230-973X.114899, PMID 24015381.
51. Hyma P, Abbulu K. Formulation and characterisation of self-microemulsifying drug delivery system of pioglitazone. Biomed Prev Nutr. 2013;3(4):345-50. doi: 10.1016/j.bionut.2013.09.005.
52. Khan S, dubey N, Khare B, Jain H. Jain PK. Preparation and characterization of alginate chitosan crosslinked nanoparticles bearing drug for the effective management of ulcerative colitis. Int J Curr Pharm Res. 2022 Sep 15;14(5):48-61. doi: 10.22159/ijcpr.2022v14i5.2040.
53. Aldawsari HM, Badr-Eldin SM. Enhanced pharmacokinetic performance of dapoxetine hydrochloride via the formulation of instantly-dissolving buccal films with acidic ph modifier and hydrophilic cyclodextrin: factorial analysis *in vitro* and *in vivo* assessment. J Adv Res. 2020;24:281-90. doi: 10.1016/j.jare.2020.04.019, PMID 32419956.
54. Samprasit W, Akkaramongkolporn P, Kaomongkolgit R, Opanasopit P. Cyclodextrin-based oral dissolving films formulation of taste-masked meloxicam. Pharm Dev Technol. 2018;23(5):530-9. doi: 10.1080/10837450.2017.1401636, PMID 29103353.
55. Naiem Raza S, Husain Kar A, Umair Wani T, Ahmad Khan N. Formulation and evaluation of mouth dissolving films of losartan potassium using 32 factorial design. Int J Pharm Sci Res. 2019;10(3):1402. doi: 10.13040/IJPSR.0975-8232.10(3).1402-11.
56. Hussain MW, Kushwaha P, Rahman MA, Akhtar J. Development and evaluation of fast dissolving film for oro-buccal drug delivery of chlorpromazine. Indian J Pharm Educ Res. 2017;51(4):S539-47. doi: 10.5530/ijper.51.4s.81.
57. Zhang L, Aloia M, Pielecha Safira B, Lin H, Rajai PM, Kunnath K. Impact of superdisintegrants and film thickness on disintegration time of strip films loaded with poorly water-soluble drug microparticles. J Pharm Sci. 2018;107(8):2107-18. doi: 10.1016/j.xphs.2018.04.006, PMID 29665377.
58. Maddela S, Buchi N, Nalluri. Development of zolmitriptan mouth dissolving films: formulation variables mechanical properties and *in vitro* drug release studies. Asian J Pharm Clin Res. 2019;12(4):273-9. doi: 10.22159/ajpcr.2019.v12i4.32176.
59. Takeuchi Y, Ikeda N, Tahara K, Takeuchi H. Mechanical characteristics of orally disintegrating films: comparison of folding endurance and tensile properties. Int J Pharm. 2020 Aug;589:119876. doi: 10.1016/j.ijpharm.2020.119876, PMID 32927004.
60. Santosh Kumar R, Satya Yagnesh TN. Oral dissolving films: an effective tool for fast therapeutic action. J Drug Deliv Ther. 2019;9(1-s):492-500. doi: 10.22270/jddt.v9i1-s.2395.
61. Cilurzo F, Cupone IE, Minghetti P, Buratti S, Selmin F, Gennari CG. Nicotine fast-dissolving films made of maltodextrins: a feasibility study. AAPS PharmSciTech. 2010;11(4):1511-7. doi: 10.1208/s12249-010-9525-6, PMID 20936440.
62. Nalluri BN, Sravani B, Anusha VS, Sribramhini R, Maheswari KM. Development and evaluation of mouth dissolving films of sumatriptan succinate for better therapeutic efficacy. J Appl Pharm Sci. 2013;3(8):161-6.
63. Tamer MA, Hammid SN, Ahmed B. Formulation and in vitro evaluation of bromocriptine mesylate as fast dissolving oral film. Int J Appl Pharm. 2018;10(1):7-20. doi: 10.22159/ijap.2018v10i1.22615.
64. Vaishali K, Bhagyashri M. Formulation and evaluation of fast dissolving oral film of buspirone hydrochloride. Int J Pharm Res. 2015;7(1):95-9.
65. Tomar A, Sharma K, Chauhan NS, Mittal A, Bajaj U. Formulation and evaluation of fast dissolving oral film of dicyclomine as potential route of buccal delivery. Int J Drug Dev & Res. 2012;4(2):408–17.
66. Husain M, Agnihotri VV, Goyal SN, Agrawal YO. Development optimization and characterization of hydrocolloid-based mouth dissolving film of telmisartan for the treatment of hypertension. Food Hydrocoll Health. 2022 Mar;2:100064. doi: 10.1016/j.fhfh.2022.100064.
67. Bichave A, Phate S, Naik V, Gaikwad A. Evaluation parameters for mouth dissolving films. Int J Pharm Sci. 2024;2(7):197-208. doi: 10.5281/zenodo.12623624.

68. Shimoda H, Taniguchi K, Nishimura M, Matsuura K, Tsukioka T, Yamashita H. Preparation of a fast dissolving oral thin film containing dexamethasone: a possible application to antiemesis during cancer chemotherapy. Eur J Pharm Biopharm. 2009;73(3):361-5. doi: 10.1016/j.ejpb.2009.08.010, PMID 19735731.
69. Senthilkumar K, Vijaya C. Formulation development of mouth dissolving film of etoricoxib for pain management. Adv Pharm. 2015;2015:1-11. doi: 10.1155/2015/702963.
70. Kokare CK, Tagalpallewar AA, Aragade PS, Bagul US, Bacchav RK, Nanjwade BK. Formulation evaluation and optimization of asenapine maleate fast mouth dissolving film. J Pharmaceut Sci Pharmacol. 2015;2(3):194-207. doi: 10.1166/jpsp.2015.1062.
71. Salamanca CH, Barrera Ocampo A, Lasso JC, Camacho N, Yarce CJ. Franz diffusion cell approach for pre-formulation characterisation of ketoprofen semi-solid dosage forms. Pharmaceutics. 2018;10(3):148. doi: 10.3390/pharmaceutics10030148, PMID 30189634.
72. Zhang H, Zhu X, Shen J, Xu H, Ma M, Gu W. Characterization of a liposome-based artificial skin membrane for *in vitro* permeation studies using Franz diffusion cell device. J Liposome Res. 2017;27(4):302-11. doi: 10.1080/08982104.2016.1231205, PMID 27581379.
73. Liu D, Zhang C, Zhang X, Zhen Z, Wang P, Li J. Permeation measurement of gestodene for some biodegradable materials using Franz diffusion cells. Saudi Pharm J. 2015;23(4):413-20. doi: 10.1016/j.jsps.2015.01.012, PMID 27134544.
74. Kalam M, Humayun M, Parvez N, Yadav S. Release kinetics of modified pharmaceutical dosage forms: a review. Contin J Pharm Sci. 2007 Jan;1:30-5.
75. Pornpitchanarong C, Akkaramongkolporn P, Nattapulwat N, Opanasopit P, Patrojanasophon P. Development and optimization of Andrographis paniculata extract-loaded self-microemulsifying drug delivery system using experimental design model. Pharmaceutics. 2024;16(2):166. doi: 10.3390/pharmaceutics16020166, PMID 38399227.
76. Kumari PV, Likhitha G, Hussain Mustaq SJ. Approach to optimize the self-microemulsifying drug delivery system for azilsartan medoxomil using box behnken design and desirability function. Int J Appl Pharm. 2024;16(2):92-100. doi: 10.22159/ijap.2024v16i2.49519.
77. Dewangan HK, Sharma R, Shah K, Alam P. Development analysis and determination of pharmacokinetic properties of a solid SMEDDS of voriconazole for enhanced antifungal therapy. Life (Basel). 2024;14(11):1417. doi: 10.3390/life14111417, PMID 39598215.
78. Iqbal WS, Chan KL. FTIR spectroscopic study of poly(ethylene glycol)-nifedipine dispersion stability in different relative humidities. J Pharm Sci. 2015;104(1):280-4. doi: 10.1002/jps.24261, PMID 25410816.
79. Farooq A, Shafaghat H, Jae J, Jung SC, Park YK. Enhanced stability of bio-oil and diesel fuel emulsion using Span 80 and Tween 60 emulsifiers. J Environ Manag. 2019;231:694-700. doi: 10.1016/j.jenvman.2018.10.098, PMID 30396142.
80. Bekhit M, Abu El-Naga MN, Sokary R, Fahim RA, El-Sawy NM. Radiation-induced synthesis of tween 80 stabilized silver nanoparticles for antibacterial applications. J Environ Sci Health A Tox Hazard Subst Environ Eng. 2020;55(10):1210-7. doi: 10.1080/10934529.2020.1784656, PMID 32614255.
81. Hydrochloride FP. Formulation and evaluation of tablets containing poorly water-soluble drug by madg method. World Journal of Pharmaceutical Research. 2017;3(16):16-25.
82. Desai ND, Mishra DS, Chaurasia R, Jat D, More MK, Soni N. Design and evaluation of self-emulsifying mouth dissolving film of ranolazine by solvent casting method. J Adv Zool. 2023;44(5)1433-45. doi: 10.53555/jaz.v44i5.4348.
83. Morakul B, Teeranachaideekul V, Limwikrant W, Junyaprasert VB. Dissolution and antioxidant potential of apigenin self-nanoemulsifying drug delivery system (SNEDDS) for oral delivery. Sci Rep. 2024;14(1):8851. doi: 10.1038/s41598-024-59617-z, PMID 38632321.